Bellcomm
955 L'Enfant Plaza North, S.W.
Washington, D. C. 20024

date: August 26, 1971

to: Distribution

B71 08038

from: R. N. Kostoff

subject: Space Shuttle and Space Tug Peak Temperatures - Case 237

ABSTRACT

Maximum Space Shuttle fuselage temperatures which occur during a typical entry are compared with maximum Space Tug temperatures during an aerobraked return from synchronous orbit to low circular orbit. Shuttle peak temperature is of the order of 2300° R assuming the heat shield to have unit emissivity. This is substantially less than the 3000 → 4500° R experienced by high ballistic coefficient ($\sim$100 lbs/ft^2) single pass aerobraked tugs and is of the same order as low ballistic coefficient ($\sim$5 lbs/ft^2) tugs. The lower shuttle temperatures are in large part due to both a lower entry velocity and lower entry angle to the sensible atmosphere than the tugs experience.

For both types of vehicles, an increase in entry angle results in higher peak temperatures at lower altitudes; an increase in ballistic coefficient has the same effect; an increase in entry velocity increases peak heating; and, for a fixed entry angle, an increase in positive L/D reduces peak temperature and increases the altitude at which it occurs.

In the general case, vehicle temperature variation in the altitude region from atmospheric entry ($\sim$400,000 ft) to the point where peak heating occurs is controlled by the slow variation of atmospheric density while temperature variation after the point of peak heating to $\sim$5,000 ft lower in altitude is controlled by the rapid variation of vehicle velocity.

(NASA-CR-121583) SPACE SHUTTLE AND SPACE TUG PEAK TEMPERATURES (Bellcomm, Inc.) 12 p

N79-72214

Unclas
00/16 12118

(PAGES) (CODE)
CR-121583
(NASA CR OR TMX OR AD NUMBER) (CATEGORY)
[redacted]

FF No. 602(A)

SEP 1971

Bellcomm

955 L'Enfant Plaza North, S.W.
Washington, D. C. 20024

date: August 26, 1971

to: Distribution

B71 08038

from: R. N. Kostoff

subject: Space Shuttle and Space Tug Peak Temperatures - Case 237

MEMORANDUM FOR FILE

Analysis

Space Shuttle Mission Profile

Reference 1 describes a typical two-stage Space Shuttle vehicle consisting of a booster, which experiences relatively low surface heating during its return to base, and an orbiter, which aerobrakes with higher surface heating. As reference 1 shows, the orbiter deboosts from low earth orbit, enters the atmosphere with flight path angle of -1.5° and speed of ∿25,200 ft/sec, holds a 60° angle of attack ($\frac{L}{D} \sim .5$, and ballistic coefficient ∿26 lbs/ft^2) through the high heating regime, then executes a landing maneuver. When the vehicle is at 60° angle of attack, maximum fuselage heating occurs on the underside immediately aft of the nose. Leading edges are not considered in this analysis.

Space Tug Mission Profile

Reference 2 describes a Space Tug which starts from synchronous earth orbit, makes one aerobraking pass through the atmosphere, and ends up in low circular orbit. The tug consists of a cylindrical core, 50 ft long x 14 ft diameter, protected by a reusable radiative heat shield. For the present study, three different heat shield configurations are examined: a hemisphere which caps one end of the cylinder, a cylinder which is concentric with, or wraps around, the core vehicle, and a flat plate which is tangent to the core vehicle cylindrical surface. The ballistic entry mode for the hemisphere configuration has flow impinging on the hemisphere parallel to the cylinder axis. For the concentric cylinder configuration, the ballistic mode has flow impinging normal to the cylinder axis. Finally, for the flat plate mounted ahead of the cylinder, ballistic entry assumes flow normal to the plate. Single-pass ballistic entry missions are examined for all the tugs, and positive and negative lift missions are included for the hemisphere-capped tug. Entry parameters for the hemisphere-capped tug include drag coefficient of unity, ballistic coefficient of 97.5 lbs/ft^2, $\frac{L}{D} = -0.3, 0.0, 0.3$, entry angles of -4.6°, -5.0°, -5.9°, and entry velocity of 33,800 ft/sec. Those for the cylindrical heat shield configuration include drag coefficient of 1.25, ballistic coefficient of 17.8 lbs/ft^2, $\frac{L}{D} = 0.0$, entry angle of -4.45°, and entry velocity of ∿33,800 ft/sec. Parameters for the flat plate heat shield configuration are drag coefficient of 1.7, ballistic coefficient of 4.0 lbs/ft^2, $\frac{L}{D} = 0.0$, entry angle of -4.03°, and entry velocity of ∿33,800 ft/sec.

Temperature Profiles

Figure 1 shows the maximum fuselage temperatures of the tugs and shuttle as a function of altitude. The vehicle surface is assumed to be in radiative equilibrium with a surface emissivity of unity, and gasdynamic radiative heating is assumed to be negligible. Starting from entry altitude, temperatures increase with decreasing altitude at similar rates for each vehicle until they peak. Below the altitude of peak temperature, which differs for each vehicle, the temperature drop precipitously for the next 5-6,000 ft. For the Shuttle, after the sharp drop has occurred, temperature continues to drop more slowly as the landing maneuver is executed. In the case of the tug, the curve terminus signifies periapsis, where the vehicle makes its closest approach to the planet surface. Past periapsis, the tug moves away from the planet, and its surface heating decreases (not shown).

Temperature Magnitudes

The Shuttle temperature peaks at ∿2,300° R at ∿255,000 ft altitude, while the peak tug temperatures range from 2200° R at 275,000 ft to 4550° R at 190,000 ft. There are several reasons for the temperature peak differences and some will be presently discussed.

One parameter, which differs for the tug and shuttle, is entry velocity. For a given vehicle, as entry velocity is increased, velocity at maximum heating increases approximately linearly.[3] Because heating is proportional to velocity cubed, a moderate increase in entry velocity will produce a large increase in heating rate. In the case of radiative equilibrium, where surface temperature is proportional to the fourth root of heating rate, the temperature increases as the 3/4 power of the entry velocity. Thus, for a shuttle entry velocity of 25,200 ft/sec, and a tug entry velocity of 33,800 ft/sec, the temperature increase due to the higher entry velocity is about 25%.

The ballistic coefficient differs among the tugs and the shuttle. According to approximate solutions in reference 3, the altitude at which peak heating occurs is proportional to $\ln \frac{C_1}{B}$, where C_1 is a constant and B is the ballistic coefficient. Thus, as Figure 1 shows for the different tugs, increasing B should decrease the altitude of peak heating. Also, as altitude of peak heating decreases, atmospheric density during peak heating increases. Because heating rate is proportional to the square root of density, heating rate will increase, and thus temperature will increase with increase in B. For the tugs, this trend is corroborated by the results in Figure 1. If the return payload of the shuttle were increased then, according to the above results, the peak temperatures would increase, and the altitude at which these temperatures would occur would decrease.

Entry angle differs for all vehicles examined. From simple geometric reasoning, it would appear that decreasing the entry angle would allow the vehicle to perform its maneuvers at higher altitudes. In fact, the approximate solutions of reference 3 show that entry angle is related to altitudes of peak heating in the same manner as ballistic coefficient. Thus, as the tug curves show, increasing entry angle forces the vehicle to experience higher peak heating at lower altitudes. An increase in the shuttle entry angle would cause an increase in peak heating at a lower altitude.

As reference 2 shows, for a tug at fixed entry angle, use of positive lift results in lower peak temperatures, while negative lift results in higher peak temperatures. Figure 2 shows that for fixed entry angle, negative lift results in lower periapsis altitude while positive lift results in higher periapsis altitude. This is reasonable, for positive lift tends to force a vehicle to higher altitudes, while negative lift tends to pull the vehicle to lower altitudes. The tug curves in Figure 1 appear to show the opposite effect, peak temperature increasing with positive $\frac{L}{D}$, and periapsis altitude decreasing with positive $\frac{L}{D}$ increase. However, it is the increase in entry angle (for the hemisphere curves) which accompanies the increase in $\frac{L}{D}$ that causes the higher heating. For fixed entry angle, use of positive lift reduces the vehicle kinetic energy which is dissipated by drag forces. Thus, to remove a given amount of energy, as is the case for a single pass aerobraking mission, the entry angle must be increased and the vehicle can then penetrate to lower altitudes. The curve terminal points in Figure 2 denote single pass missions, and clearly show how periapsis altitude decreases with increasing lift.

Vehicle shape has a major influence on surface heating. An increase in radius of curvature results in a decrease in local convective heating. Thus, a flat plate heat shield has less surface heating than a sphere of similar cross-section. Also, a cylinder has 73% of the stagnation heating rate of a similar diameter sphere. Thus, there is a separation between the tug curves on Figure 1 due to a configuration effect. The shuttle region of maximum heating is relatively flat, resulting in low fuselage heating rates.

Temperature Gradients

The shape of the temperature curves in Figure 1 from atmospheric entry to slightly beyond the point of peak heating will now be more closely examined.

Stagnation point convective heating Qs may be written as[3]

$$Qs = C\rho^{1/2}V^3 \tag{1}$$

where C is a constant, ρ is local atmospheric density, and V is vehicle velocity.

With the assumption of radiative equilibrium, convective heat flux Qs may be equated to energy radiated from the heat shield surface to yield a surface temperature Ts

$$Qs = \varepsilon\sigma Ts^4 \tag{2}$$

where ε is the surface emissivity, and σ is the Stefan-Boltzmann constant. Equate (1) to (2) to get:

$$Ts = C^1 \rho^{1/8} V^{3/4} \tag{3}$$

where C^1 is constant.

Density may be written, assuming an exponential atmosphere[3], as

$$\rho = \rho_o \, e^{-\frac{z}{H}} \tag{4}$$

where z is altitude, ρ_o is atmospheric density at z=o, and H is atmospheric density scale height and may be taken as 22,500 ft.[3]

An expression for velocity is obtained by curve fitting the velocity-altitude plots of Figure 3. These curves apply to the tug with hemispherical heat shield in both a lifting and ballistic mode, but are similar to the other tugs and the shuttle as well. They are represented mathematically by the equation:

$$V(Z) = V_e \left(1 - \left[\frac{V_e - V_p}{V_e} \right] e^{-3.5 \frac{(Z-Zp)}{H}} \right) \tag{5}$$

where V_e is entry velocity (Z=400,000 ft.), V_p is periapsis velocity, and Zp is periapsis altitude.

Temperature T_s may now be written as

$$T_s = C_k \, e^{-\frac{z}{8H}} \left(1 - \left[\frac{V_e - V_p}{V_e} \right] e^{-3.5 \frac{(Z-Zp)}{H}} \right)^{3/4} \tag{6}$$

where C_k is a constant.

It is the product of two terms, and its variation is the product of the variation of each term. The density factor $e^{-\frac{z}{8H}}$, causes temperature to decrease with increasing altitude, with an e-folding distance (distance in which a quantity changes by 1/e) of 8H, or 180,000 ft. The velocity

factor, $\left(1 - \frac{V_e - V_p}{V_e} e^{-3.5 \frac{(z-z_p)}{H}}\right)^{3/4}$, causes temperature to

increase with increasing altitude, with an e-folding distance of 7,000 ft. from periapsis. Thus, starting from periapsis and proceeding higher in altitude, the temperature increases rapidly due to the velocity term, peaks when the velocity term is of the same order as the density term, then decreases slowly with altitude as it follows the density term. The region of deviation of the temperature curve from the exponential density dependence, $e^{-\frac{z}{8H}}$, near periapsis is about 8,000 ft, which is of the order of the e-folding distance due to velocity change. Also, at higher altitudes, the slope of the temperature curve follows the slope of the density curve, and increases with increasing altitude.

Materials for Thermal Protection Systems

On the left hand portion of Figure 1 are printed candidate heat shield materials, where the tic adjoining each material name denotes the maximum recycling temperature which the material could withstand operating in a reusable mode.[4] These materials are assumed to require coating for purposes of oxidation resistance.

The peak heating region of the shuttle is slightly above the Inconel range, but safely within the domain of Columbium. This statement applies as well to the flat plate tug heat shield. For the concentric cylinder, Tantalum may be utilized in a conservative design. Finally, for the hemispherical tug heat shields, practical design necessitates utilization of high temperature materials, such as the ZrB_2 alloy mentioned on Figure 1, or a Carbon-Carbon alloy.

R N Kostoff

1013-RNK-ajj pjr

R. N. Kostoff

REFERENCES

1. Faget, M., "Space Shuttle: A New Configuration," Astronautics and Aeronautics, January 1970, P-52.

2. Kostoff, R. N., "Aerobraking the Space Tug from Synchronous Orbit into Low Circular Earth Orbit: Guidance and Heating Constraints on First Atmospheric Pass," Bellcomm Memorandum for File, July 15, 1971.

3. Martin, J. J., "Atmospheric Reentry," Prentice-Hall, Inc., Englewood Cliffs, New Jersey, 1966.

4. Ong, C. C., "Radiative Thermal Protection System Materials for Reusable Reentry Vehicles," Bellcomm TM-70-1013-3, March 6, 1970.

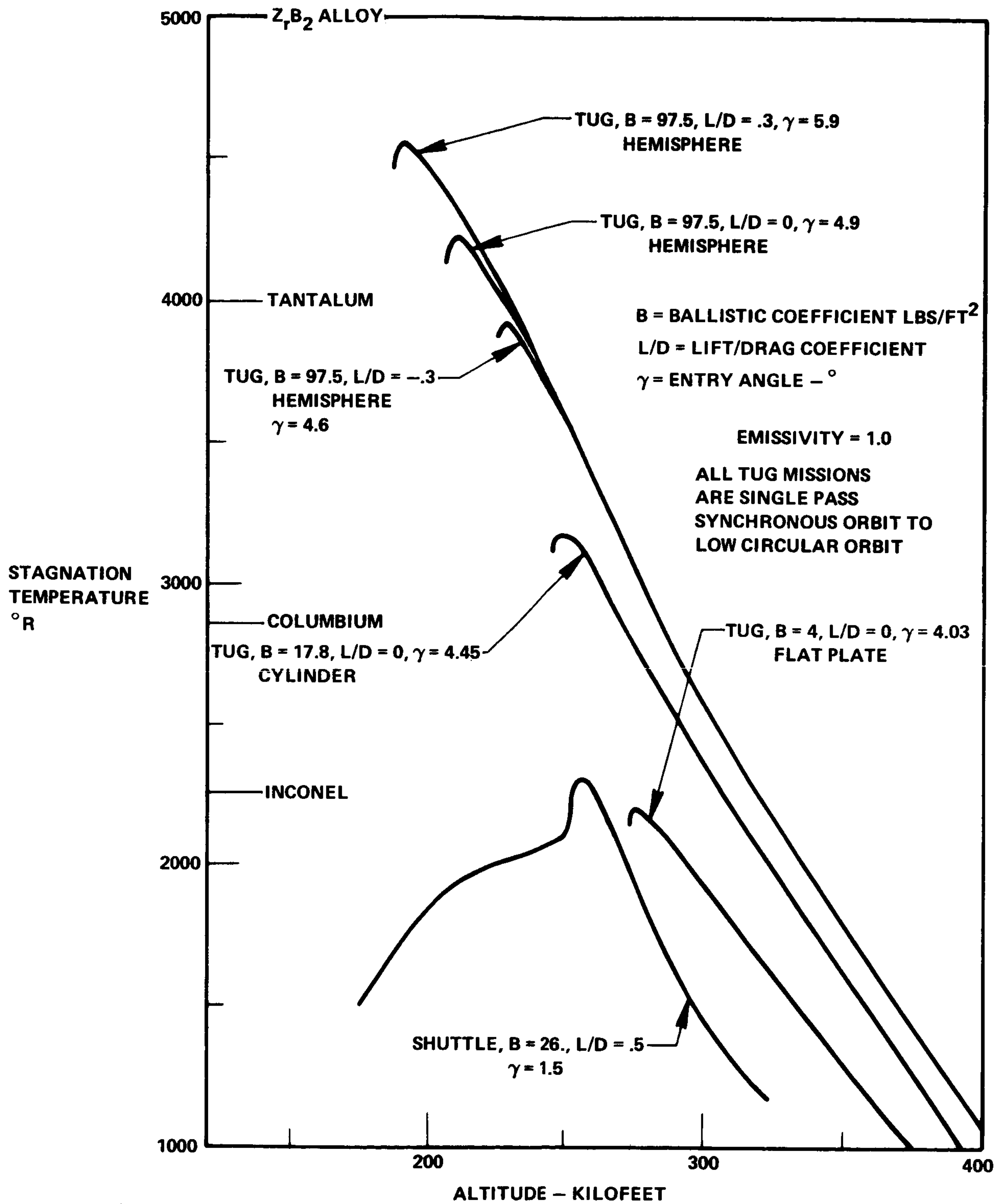

FIGURE 1 - MAXIMUM TEMPERATURES ON TUGS AND SHUTTLE VS ALTITUDE

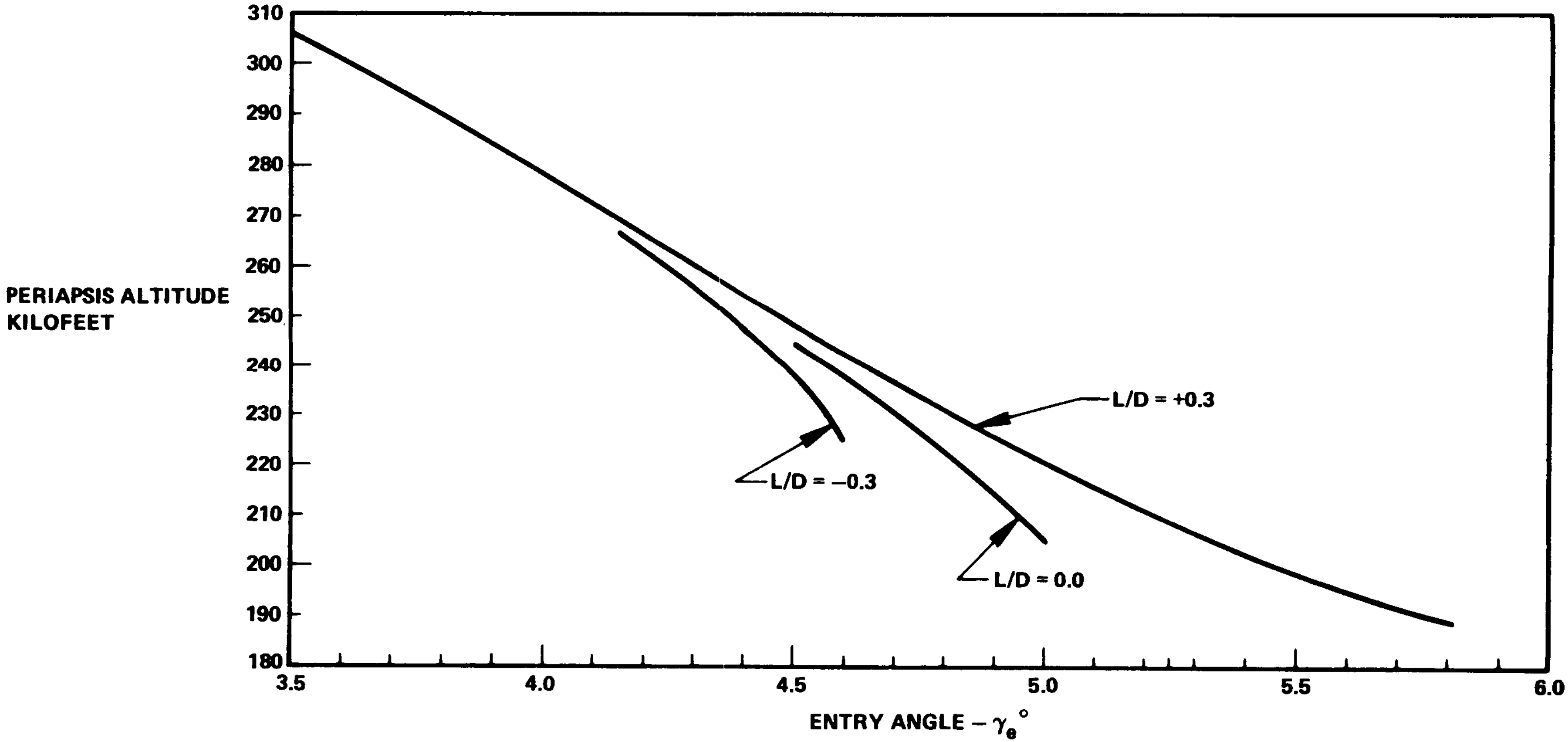

FIGURE 2 - PERIAPSIS ALTITUDE VS. ENTRY ANGLE

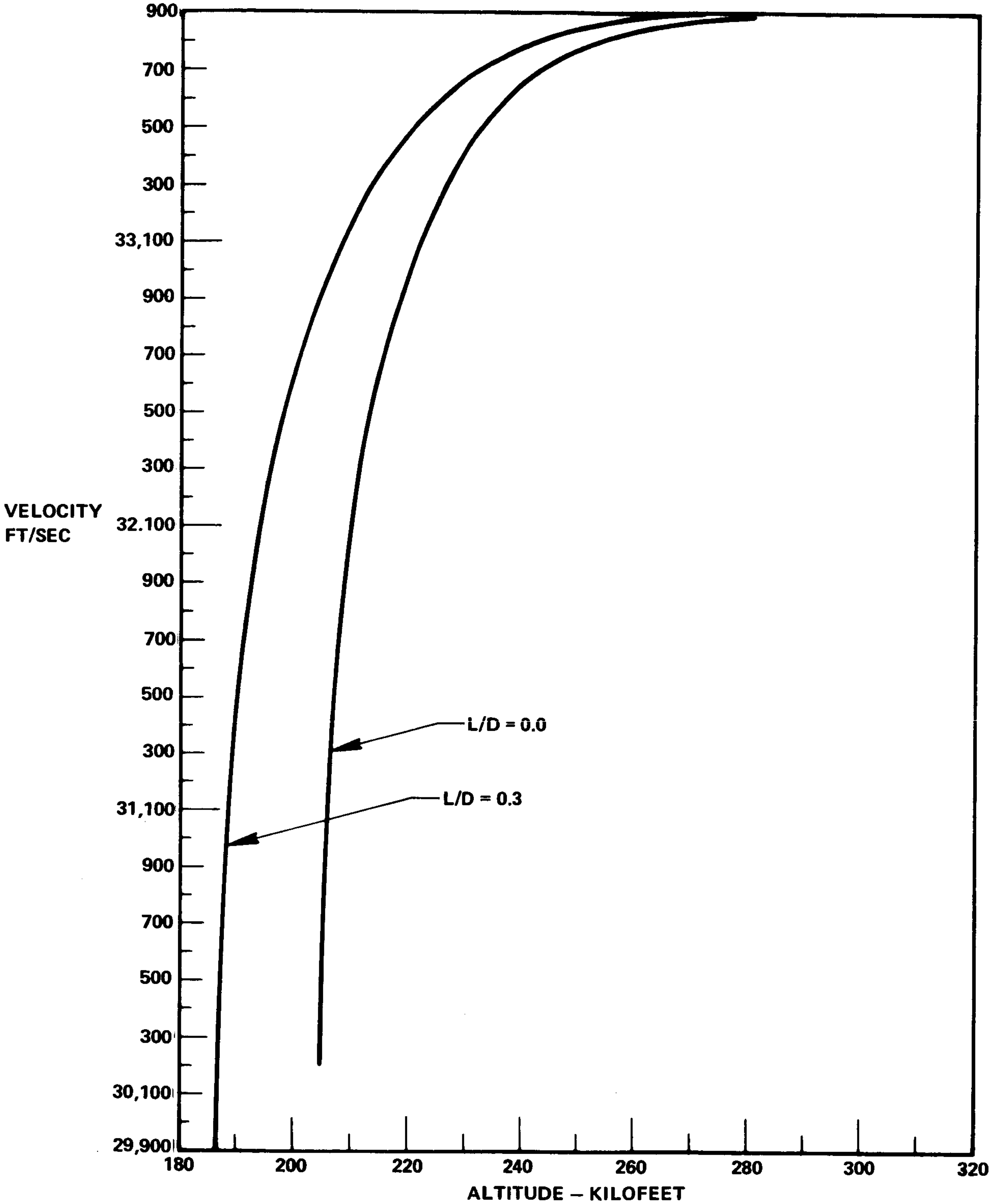

FIGURE 3 - VELOCITY VS. ALTITUDE

Subject: Space Shuttle and Space Tug Peak Temperatures - Case 237

From: R. N. Kostoff

DISTRIBUTION

NASA Headquarters

W. O. Armstrong/MTX
P. E. Culbertson/MT
L. E. Day/MH
F. J. DeMeritte/RV-1
G. C. Deutsch/RW
C. J. Donlan/MD-T
E. W. Hall/MTG
V. N. Huff/MTE
M. Kitchens/MTE
A. S. Lyman/MR
M. F. Markey/MTG
N. G. Peil/MH
L. R. Scherer/MAL
A. D. Schnyer/MTE
A. O. Tischler/RS
J. W. Wild/MTE

KSC

M. Cardone/LV-TMU-A
H. Clark/FP-B

LaRC

E. S. Love/227B
E. B. Pritchard/213A
A. S. Schy/152B

MSC

J. Funk/FM8

MSFC

T. Barret/PD-SA-V
R. Burns/S&E-AERO-GT
R. J. Corcoran/PD-RV
E. Dickmanns/S&E-AERO-NAS-NRC
J. Furman/S&E-ASTN-AA
E. Stuhlinger/AD-S
E. Teague/S&E-AERO-P
B. Wales/PD-DO-S

Bellcomm

G. M. Anderson
A. P. Boysen
D. R. Hagner
J. Z. Menard
J. W. Timko
M. P. Wilson
All Members Depts. 1011, 1013
Central Files
Department 1014 Supervision
Department 1015 Supervision
Department 1024 File
Library

Abstract Only to

J. P. Downs
D. P. Ling
R. L. Wagner